Calculated photoemission spectra from the Al(001) surface

Shih-Kuei Ma and Kenneth W.-K. Shung
Department of Physics, National Tsing Hua University, Hsinchu, Taiwan 30043, The Republic of China
(Received 2 August 1993; revised manuscript received 22 November 1993)

We present a theoretical study of photoemission from the Al(001) surface. The purpose of this work is to examine the validity of the nearly-free-electron-gas model for Al, and to study the importance of many-body and surface effects in its photoemission spectra. This is an extension of our earlier study on the Na spectra, but the band structure of Al is much more complicated and requires a detailed band calculation. A slab model is employed to self-consistently determine its band—with the inclusion of the self-energy correction. The band states are then used to calculate the photoemission spectra, which are compared with measurements. Reasonable agreement has been found for the Al bandwidth, and also for the spectral profiles at various photon energies. This result strongly supports the view that, once the many-body and surface effects are properly taken into account, the spectra can be well described with the nearly-free-electron bands—as in the case of Na. Special attention has been paid to surface-state emissions. A resonant enhancement in its spectral intensities has been found both in the calculation and in the measurement. However, there still exist some discrepancies which call for further studies.

I. INTRODUCTION

There have been persistent interests in the band structure of simple metals and in the validity of the nearly-free-electron (NFE) model for these metals. On the theoretical side, detailed theories,[1-5] which include the many-body effects, exist for the NFE model. Simple metals, thus, provide us a unique opportunity to examine the theory. On the experimental side, the problem was revived due to the improved resolution in the angle-resolved photoemission spectroscopy, which is generally regarded as the most direct method for band measurements. Recent photoemission studies by Plummer and co-workers, however, have revealed serious discrepancies between the theory and the measured band structures of Al,[6] Na,[7,8] and K.[9] These negative results cast serious doubts on the existing theories for simple metals. In this work, we calculate the Al spectra based on the NFE model and compare the results with experiments. This is an extension of our earlier studies on the spectra of Na.[10-14] The band structure of Al, however, is more complicated and hence requires a careful band calculation to begin with. Our main conclusion is that, for both Na and Al, the measured spectra can be reasonably well explained with the NFE model, provided that the many-body effects (i.e., the self-energy, $\Sigma=\Sigma_1+i\Sigma_2$) and the surface effects are properly taken into account.

The importance of these effects are, however, usually neglected in photoemission analysis. Peaks in spectra are normally associated with vertical transitions between bands;[6-9] i.e., transitions that conserve both the energy and the crystal momentum of the electrons. The importance of the surfaces and the complex self-energy is that the momentum needs not be strictly conserved in photoexcitations. They could thus appreciably modify the peak positions and the spectral profiles. These effects should not be neglected.

A brief review on the spectra of Na and K is appropr ate when addressing the issues involved here. Plummer, and co-workers have found that [7,8] the occupied bandwidth of Na is narrower than the NFE prediction by 18%, and that there are anomalous Fermi-level peaks that cannot be explained with vertical transitions between the NFE bands. The self-energy correction (Σ_1) is known to cause some bandwidth narrowing in Na, but it can only account for about one half of the observed narrowing effect.[1,3,4] Shung and Mahan[10,11] (SM) performed a detailed calculation for Na and showed that the imaginary part of the self-energy (Σ_2) is crucial to this problem. Its importance is twofold. One is that the states are broadened by Σ_2 and, hence photoexcitations need not be strictly vertical within this energy resolution. The other is that the mean free path (MFP), which equals $-v_k/2\Sigma_2$, of Na is only about 5 Å. The short MFP makes photoemission very sensitive to the surface potential, since most photoelectrons are coming out from the first few layers of Na(110). SM showed that the bandwidth does "appear" narrower in the spectra—in agreement with the measurements. It only "appears" so since the peak positions have been shifted from where allowed by vertical transitions. The shift is a consequence of the short MFP and the surface-induced emissions. The same combined effect has also been found to cause the anomalous Fermi-level peaks, and our study has correctly predicted the spectral strength of the peaks as a function of the photon energy. So, SM's study indicates no major discrepancies between the Na photoemission spectra and the NFE model. The problem is with the straightforward vertical-transition analysis which overlooks the importance of the many-body effect and the surface effect in photoemission. We note that there are other explanations[15,16] concerning the Na spectra, but these explanations need detailed calculations for the photoemission matrix elements to substantiate their claims.

Both K and Na have the monatomic bcc structure and they differ mainly in their lattice constants. These two

0163-1829/94/49(15)/10617(9)/$06.00

metals are thus expected to share common features in their photoemission spectra. Indeed they do, but there are discrepancies[9] which might suggest problems with applying SM's explanation to other simple metals. Measured[9] bandwidth of K is 25% narrower than the NFE band—in close agreement with the calculations.[11] Agreements were also found on the position of the anomalous peaks, but *not* on their intensities. This discrepancy is serious. According to SM's theory,[11] the peak intensity should reduce at $\hbar\omega=20-30$ eV since the peaks correspond to nonvertical transitions. In fact, the peak intensities were found to increase like a broad resonance in this energy range. So far, no theory has been established to explain this result.

It is clear that an investigation on the validity of SM's photoemission theory in different simple metals is important. The present study concerns the spectra from the Al(001) surface, for which detailed measurements[6] are available for comparison. Being a trivalent metal, Al has a complicated band structure below E_F. The band in the [001] direction has a measured energy gap of 1.68 eV in width at 1.99 eV below E_F and there are surface states inside this gap. The surface states are of special interests here since their spectral profiles are very sensitive to the surface-related effects that SM have found important in photoemission.

The band of Al in the [001] direction is self-consistently determined with the use of the density-functional formalism.[17] A slab model[18] has been employed in which the averaged lattice potential on the [001] planes were taken. By doing this, we achieve a good description of the surface profile and the band structure; meanwhile, we are still able to include the self-energy correction that SM have suggested to be important. The calculated band states are employed to evaluate the photoelectron intensity. We expect this method to be valid for normal and near-normal emissions from the Al(001) surface. The calculated spectra are found in reasonable agreements with the measurement,[6] in the peak positions, the spectral line shape and also in the size of the bandwidth reduction from the NFE band. So the major improvement of this study over SM's analysis is to employ realistic Bloch states for calculations. Such a practice is essential for Al due to the complicated Al bands. There are indications that similar band effects could also modify the spectra of Na and K, especially for states near the Fermi level.

The surface state has been determined numerically. The calculated spectral intensity of this state shows a resonant enhancement at $\hbar\omega=76$ eV—in agreement with the measurement. However, the calculated surface-state cross section is considerably larger than the measured result on the low-energy side of the resonance. They differ, for example, at $\hbar\omega=50$ eV by a factor of 30. A two-band analysis has been employed for a closer look at this discrepancy. This is an analytical calculation and the result shows a similar discrepancy when compared with the measurement. It is not clear what might have caused the large difference.

Briefly, the calculated spectra of Al show reasonable agreements with the measured ones. This finding provides further support for the view that the NFE model is reasonable for the simple metals. The result once again illustrates the importance of the many-body and surface effects in photoemission spectroscopies. The calculations and results are discussed in detail in the next section, which is followed by the concluding remarks. The appendix contains the analytic two-band analysis, where an emphasis was put on the surface states and the states near the energy gap.

II. CALCULATION AND DISCUSSION

In this work we extend the study of SM to the photoemission spectra from the Al(001) surface.[6] As in SM, we employ Mahan's theory of photoemission.[19] The quantity to be calculated is the emitted current per solid angle, per energy. The momentum parallel to the metal surface is assumed to be conserved; then, the normal-emission (say, in the z direction) spectra can be expressed by

$$\frac{dI}{dE_p d\Omega} \propto \frac{\sqrt{E_p}}{\omega^3} \sum_k \left| \left\langle \psi_p^> \left| \frac{dV(z)}{dz} \right| \psi_k \right\rangle \right|^2 A_k(E_p-\hbar\omega) , \tag{1}$$

where k is summed over all occupied states along the $\Gamma\rightarrow X$ direction. The quantity $\hbar\omega$ is the photon energy, $E_p=p^2/2m$ the photoelectron energy measured externally, and $V(z)$ the effective potential in the direction normal to the surface. Unless otherwise noted, energy zero is always referred to $V(z)$ at $z\rightarrow\infty$; for example, the work function equals $-E_F$ in this energy scale. ψ_k is the initial state and $\psi_p^>$ the scattered wave in the final state; $d\Omega$ is a small solid angle in the normal direction of emission. $A_k(\epsilon)$ is the spectral function of destroying a k-state electron at the energy ϵ:

$$A_k(\epsilon)=\sum_s |\langle s|\hat{c}_k|0\rangle|^2\delta(\epsilon+E_s-E_0) ,$$

where $|s\rangle$ denotes an $(N-1)$-electron state with the energy E_s, $|0\rangle$ is the N-electron ground state at E_0 and $\hat{c}_k$ the annihilation operator of the state ψ_k.

The screening of the electromagnetic field is neglected in this work. In general, this screening effect is very important in the surface region at low frequencies, but its importance decreases rapidly as $\hbar\omega$ is increased beyond the plasmon energy.[20] At $\hbar\omega=50$ eV, for example, the unscreened field is estimated to deviate from the screened one by less than 10% in magnitude. Neglecting the screening effect is reasonable here since our discussions are mostly in the $\hbar\omega>50$ eV regime.

Two features that distinguish the Al band from the simple Na band are (a) the presence of an energy gap below the Fermi energy E_F and (b) the existence of a surface state inside the gap. A detailed band calculation that goes beyond the jellium model is therefore, necessary. The details of the Al band calculation are discussed in Sec. II A for the band states and Sec. II B for the surface state; which are followed by a discussion on the calculated spectra in Sec. II C.

A. The band states

A slab model[18] is used here for a self-consistent band calculation, in which the density-functional theory within the local-density approximation[17] has been employed. In the slab model, the lattice potential is averaged over the [001] lattice planes. This is consistent with Eq. (1) where nonvertical Bragg scattering has been neglected.

The Ashcroft pseudopotential, which has a soft core of radius r_c, is used here to describe the lattice potential. After the layer averaging, the potential from a layer located at $z=0$ has the form:

$$V_{\text{pseudo}}(z)=\begin{cases}2\pi e^2 dn r_c\ , & |z|<r_c\\ 2\pi e^2 dn|z|\ , & |z|>r_c\ ,\end{cases} \tag{2}$$

r_c is the 1.12 Bohr radius (a_B) for Al.[21] The averaged electron density is $n=(4\pi r_s^3/3)^{-1}$ with $r_s=2.07a_B$, and $d=3.82a_B$ denotes the spacing between the [001] planes in Al. Equation (2) gives the unscreened lattice potentials: $V_{002}=0.91$ eV and $V_{004}=0.73$ eV, which remain unchanged from their respective values before the layer averaging. We employed a slab that contains 20 layers of Al atoms for a self-consistent band calculation. The lattice relaxation on the Al(001) is small[22] and is, hence, neglected.

The slab model is employed here for the sake of quick convergence in calculation. This method is believed to produce a good description both at the surfaces and in the interior of the bulk Al.[23] Figure 1 illustrates the calculated effective potential $V_s(z)$; where the subscript indicates the slab model. The first layer atoms have been placed at $z=-d/2$. The result agrees reasonably with other similar calculations.[23] There is a surface-potential barrier of height $V_0=15.95$ eV, which corresponds to a work function of 4.20 eV—in reasonable agreement with the measured value of 4.41 eV.[24]

$V_s(z)$ clearly becomes periodic beyond the first few layers near the surface. It is thus convenient to modify the slab potential for the description of a semi-infinite sample (in the $z<0$ half-space by assumption) simply by duplicating the tenth layer potential for all the subsequent layers until $z\to-\infty$. We will use this modified potential in the following calculations but will still denote it by $V_s(z)$. We note that the screening of the lattice potential and the surface potential are readily built into $V_s(z)$. With the use of this modified slab potential, the momentum of a state can be easily defined (see later). This is very important since, after all, it is the energy dispersion as a function of momentum we want to examine in photoemission.

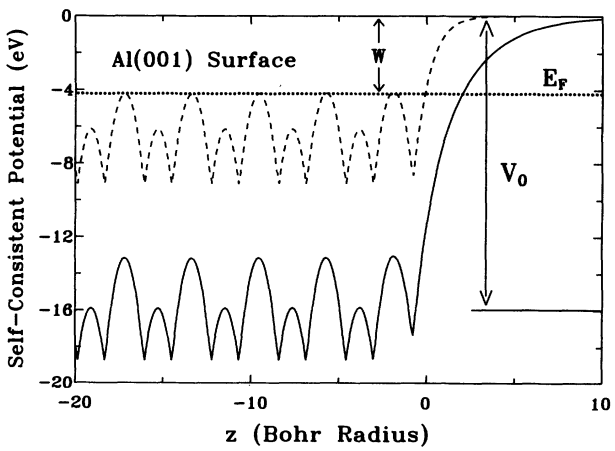

FIG. 1. The first ten layers of the calculated Al(001) surface potential. The solid curve is the total effective potential, the dashed curve the Hartree potential. The Fermi level is indicated by the dash-dotted curve. The calculated work function is $W=4.20$ eV and the surface potential step is 15.9 eV.

Wave functions are needed to evaluate the photoexcitation matrix elements in Eq. (1). States directly determined from V_s are, however, not suitable here; since the self-energy correction (Σ_1) is our main concern but has not been included. A procedure is needed to generate states such that quasiparticle states, ψ_k or $\psi^>$, have the correct relation between their external energy E_p, and their crystal momentum k inside the solid. For example, a state at $E_p>0$ should oscillate like $e^{\pm ipz}$ for $z>0$ and like $e^{\pm ikz}$ for $z\ll 0$. Since the self-energy correction inside the metal is k dependent, the wave functions are to experience a k-dependent (or an energy-dependent) surface-potential barrier.[12] We thus employ a method used in Ref. 12 and assume that the quasiparticle wave functions are given by an effective Schrödinger equation:

$$[T+V_H(z)+V_{\text{xc}}(E,z)]\psi_E(z)=E\psi_E(z)\ , \tag{3}$$

where T stands for the kinetic-energy operator, $V_H(z)$ is the static Hartree potential (i.e., the dashed curve in Fig. 1), and $V_{\text{xc}}(E,z)$ an energy-dependent exchange-correlation potential. We further assume that $V_{\text{xc}}(E,z)$ is real and proportional to the Kohn-Sham exchange-correlation potential $V_{\text{xc}}(z)$, i.e.,

$$V_{\text{xc}}(E,z)=f(E)V_{\text{xc}}(z)\ , \tag{3'}$$

where $f(E)$ is to be determined. Effectively, the complex, nonlocal effective-mass operator[17] of the quasiparticle states has been approximated by a real, local one in Eq. (3). With this approximation, the calculations are kept simple enough so that the one-body characters of quasiparticles can be clearly identified in the analysis.

The energy-dependent scaling factor $f(E)$ is determined with the application of the jellium model. Deep inside the jellium, states have a well-defined momentum k. Within the Kohn-Sham scheme the density-functional calculation would yield $f(E)=1$ and $V_s(z)=V_H(z)+V_{\text{xc}}(z)$, and $\lim_{z\to-\infty}V_{\text{xc}}(z)=\Sigma_1(k_F)$.[17] If the self-energy correction is included, it follows from Eqs. (3) and (3') that ($\hbar=m=1$)

$$E_k=k^2/2-\phi+f(E)V_{\text{xc}}(-\infty)=k^2/2-\phi+\Sigma_1(k)\ ,$$

where $\phi=V_H(-\infty)$ is the Coulomb barrier due to the charge redistribution at the surface. The jellium model thus suggests

$$f(E)=\frac{\Sigma_1(k)}{\Sigma_1(k_F)}\ , \tag{4}$$

which is employed in the following calculations. The

method is expected to work fairly well for simple metals like Al, since the lattice potential of which is weak. The k-dependent self-energy is calculated using the Rayleigh-Schrödinger method and the result for $0<k<5k_F$ has been given in Ref. 12. The self-energy correction leads to a 0.22-eV conduction bandwidth reduction in Al. This value agrees reasonably well with the random-phase-approximation results of 0.20 eV (Refs. 1 and 3) (see discussion later). The Rayleigh-Schrödinger method has been applied with success to the polaron problem[25] and heavily doped semiconductors.[26]

Both the wave functions and the density of states of the occupied states are needed in evaluating Eq. (1). These states have $E<0$ and the wave functions are thus real. The wave functions must be expressible as combinations of Bloch waves $[u(z+d)=\exp(ikd)u(z)]$ deep inside the crystal; i.e., the solutions of Eq. (2) have the form

$$\psi_E(z)=u(z)+u^*(z)\ ,\quad z\ll 0\ . \tag{5}$$

After a few steps of simple algebra, we obtain

$$\cos(kd)=\frac{\psi_E(z+d)+\psi_E(z-d)}{2\psi_E(z)}\ . \tag{6}$$

This equation uniquely determines the relation between the external energy E of an electron and its crystal momentum k inside the crystal—with the band structure effect, the surface, and the self-energy correction all taken into consideration. Ordinary band calculations do not include the self-energy correction.[5]

Band states are those with real k or, equivalently, with the absolute value of the right-hand side of Eq. (6) less than 1. The band structure obtained this way is shown by the dots in Fig. 2; where the Fermi energy is put to zero. The density of states is easily determined from the dispersion of the band. This calculation agrees excellently, except near the zone boundary, with a quasiparticle band (dashed curve) defined by: $C+k^2/2m+\Sigma_1(k)$, where C is a constant energy shift to align the Fermi energy to zero. At the zone boundary there is a 1.7-eV band gap in the calculated band structure. This gap size is slightly less than $2V_{002}$ because of the screening effect. The calculated band in the gap region can actually be well approximated with a simple two-band analysis if a lattice potential $2V_G=1.7$ eV is employed. The two-band method is summarized in the Appendix, which is useful for later analysis. The calculated gap size agrees closely with the measured result[6] of 1.68 ± 0.08 eV. The NFE band without the self-energy correction is given by the solid curve, which has a bandwidth of 11.69 eV. There is a small $[\Sigma_1(0)-\Sigma_1(k_F)=0.22$ eV] bandwidth narrowing effect due to the self-energy correction. The measured bandwidth reduction is 1.1 eV.[6] The difference in the quasiparticle bandwidth and the measurement is partly due to photoemission itself; which is discussed in Sec. II C.

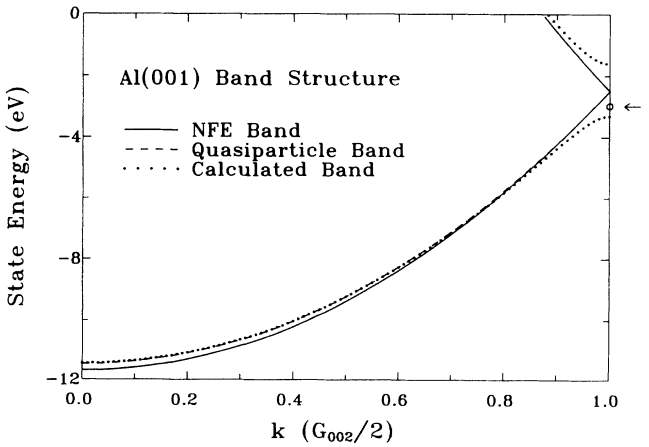

FIG. 2. The Al band structure in the [001] direction. The solid curve is the NFE band, and the dashed curve is the quasiparticle band where the self-energy correction has been included. The dots indicate the evaluated band which also includes the lattice scattering. This calculated band agrees with the quasiparticle band except at the zone boundary where a gap opens up. The open circle at -2.98 eV indicates the surface state. k is measured in units of $G_{002}/2$.

B. The surface state

Surface states are Bloch states with complex wave vectors; they can thus only exist at surfaces. A simple two-band analysis (see Appendix) shows that the surface state on the Al(001) surface has a crystal momentum $k=\pi/d-iq$. By approximating the surface potential by a step potential of height V_0, we have found that $q=0.07$ (1/Å).

Equation (6) is valid for a surface state too; but the absolute value of the cosine function is now greater than one because of the complex k. The absolute value of the right-hand side of Eq. (6) is always greater than one inside the gap. We, therefore, need to use a different criterion to locate a surface state. A quantity $\gamma_E(z)=\psi_E(z)/\psi_E(z+d)$ is defined first. A surface state is located where $|\gamma_E|<1$ and $\gamma_E(z)$ agrees with $\gamma_E(z-d)$ to within 0.01%. The self-energy of the surface state is expected to be small since $\Sigma_1(\pi/d)-\Sigma_1(k_F)=5\times10^{-3}$ eV, which is negligible, and $\Sigma_2(\pi/d)=0.04$ eV. The Al(001) surface state is found at 2.98 eV below E_F (shown by the arrow in Fig. 2). This value agrees closely with that from the two-band model (at 2.6 eV) and that by measurement (at 2.75 eV).

We remark that, as far as photoemission is concerned, a surface state is very similar to a band state near the gap. They are close in energy and also in momentum. The imaginary part of the surface-state momentum could be irrelevant if the inverse of it is much larger than the MEP of the photoelectron. For the Al(001) surface state, $\hbar/q\sim14$ Å and the MFP is about 4 Å. The "vertical" transition from the surface state would thus be analogous to that from a state near the band edge.

C. The calculated spectra

The spectra can now be evaluated using Eq. (1) with the band and the surface states determined in the previous subsections. The final state, $|\psi_p^>\rangle$, represents a scattered wave which is determined numerically in accor-

dance with Eqs. (3) and (4). The Coulomb scattering is taken into account by including Σ_2 in the potential. The procedure is similar to that employed in the low-energy-electron-diffraction (LEED) state calculation.[27] The initial and final states, whether they are bandstates or are in a gap, can be analytically studied within the two-band model, which is summarized in the Appendix. These analytic results are very useful for checking the validity of our numerical calculations. For instance, the numerically generated surface state wave function is found well described by Eqs. (A6)–(A8).

The self-energy does not depend on energy within the Rayleigh-Schrödinger approximation; therefore, the spectral function can be expressed by a Lorenzian:

$$A_k(\epsilon)=\frac{1}{\pi}\frac{-\Sigma_2(k)\Theta(E_F-\epsilon)}{(\epsilon-E_k)^2+\Sigma_2^2(k)} .$$

E_k is the one-body state energy defined by Eq. (3). A small surface-state broadening effect, which is approximated by $\Sigma_2(\pi/d)=0.04$ eV, has been included in the following calculation.

The calculated spectra at selected photon energies are given as functions of the initial-state energy in Fig. 3, where we have aligned E_F to zero. A Gaussian of full width 0.5 eV has been included to account for the instrumental broadening.[6] The result can be directly compared with the measurement of Levinson, Greuter, and Plummer (Fig. 4 of Ref. 6). Both the calculation and the measurement show similar spectral features: the peak structures can be grouped into three energy regions. The stationary peak at ~ -3 eV is due to the surface state. The peak structure to the left of the surface state comes mainly from the vertical transitions. Peaks also appear to the right of the surface state. These high-energy structures are mostly due to the same surface effect that explains[10,11] the anomalous peaks in the Na spectra. The spectral characters at these three energy regions are, respectively, discussed below.

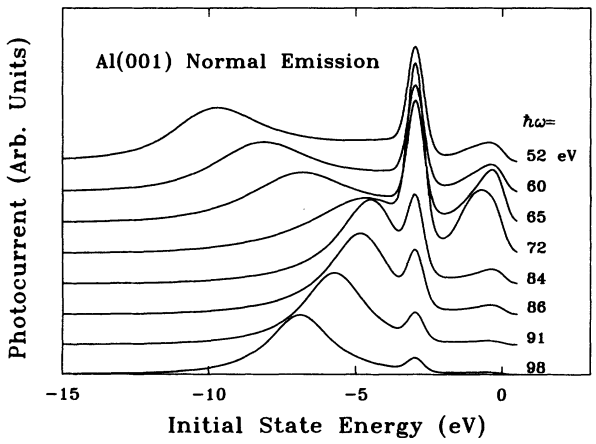

FIG. 3. Calculated normal-emission spectra at different photon energies are illustrated here. The spectra are given in terms of the initial-state energy. A 0.5-eV instrumental broadening effect has been applied to the spectra.

A typical spectrum is shown in Fig. 4 for $\hbar\omega=44$ eV (the solid curve), where the three main structures described above can be easily identified. An attempt has been made here to differentiate various contributions due to, respectively, the periodic bulk potential (the dotted curve), the surface (the dashed curve), and their interference (the dot-dashed curve). This is achieved by separating $V_s=V_{\text{bulk}}+V_{\text{surface}}$ in calculating

$$\left|\left\langle\psi_p^{>}\left|\frac{dV_s(z)}{dz}\right|\psi_k\right\rangle\right|^2$$

of Eq. (1). Recall that $V_s(z)$ has been made periodic by duplicating the tenth layer potential to the subsequent layers. V_{bulk} can thus be defined accordingly by repeating the tenth layer potential for all layers and putting $V_{\text{bulk}}(z)=0$ for $z>0$. The difference between V_s and V_{bulk} then gives V_{surface}. The separation of the surface and the bulk contributions here is somewhat artificial, since the wave functions have been determined in accordance with $V_s(z)$ and hence contain both the surface and the bulk characters. This differs from SM's calculation where the wave functions are determined within the jellium model and, hence, do not contain the lattice contribution. This difference explains the appearance of the two bumps in the dotted curve at ~ -0.5 and -3 eV, which is additional to the vertical transition at ~ -11 eV. The large size of the ~ -0.5-eV structure clearly suggests that photoemission spectra cannot be fully understood by means of the vertical transitions alone.

The structure at ~ -0.5 eV in Fig. 4 has nothing to do with vertical transitions at all. It is induced by the nonperiodic surface potential. The same surface effect has been found by SM to cause the anomalous structure at E_F in the Na spectra. Here in the spectra of Al, the sur-

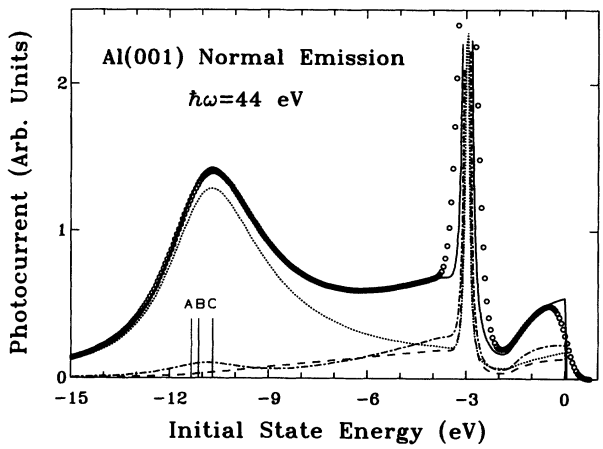

FIG. 4. A typical spectrum at $\hbar\omega=44$ eV (the ○ point) is examined. The spectrum before the instrumental broadening is shown by the solid curve, which is decomposed into a surface-induced part (the dashed curve), a lattice contribution (the dotted curve), and an interference term (the dash-dotted curve). The short, vertical lines, respectively, indicate the expected vertical transition position of the NFE band (A), the quasiparticle predicted peak position (B), and the actual peak position from the calculation (C).

face effect is mainly to cause an edge at E_F in the spectra, which appears in a peak form since there is an energy gap ~ 2 eV below E_F. This surface-induced peak structure makes it difficult to determine the band dispersion of the upper part of the conduction band. Vertical transitions from these states are possible at $\hbar\omega \sim 68-82$ eV, but their peak positions are strongly modified (see Fig. 5 later) by the surface effect, which is intrinsic to photoemission so it cannot be discarded. However, the surface effect reduces rapidly as the photon energy increases[10,11]—as is seen clearly from Fig. 3 and also from the measurement. Thus, it would be better to determine the upper part of the conduction band at higher photon energies.

The photoexcitations from the bottom part of the conduction band (e.g., the -11-eV structure in Fig. 4) are closely related to the vertical transitions, but their peak positions have been modified. The modification causes difficulties in the band determination: it usually makes the bandwidth appear narrower than it actually is. The letter A in Fig. 4 indicates the expected vertical transition peak position of NFE band. The predicted peak position of the quasiparticle band is, in fact, at B. The apparent peak position is found at C, which is about 0.4 eV above B. The peak position is modified from the position predicted by quasiparticle band for two main reasons: (1) the potential is nonperiodic in the surface region, which makes strict momentum conservation unnecessary; (2) states near the band bottom are broad in width ($\Sigma_2 \sim -1.2$ eV), which enhances the importance of the nonvertical transitions. We have found that these effects usually shift the peak positions upwards in energy,[10,11] and that the shift is most apparent near the band bottom. There is a simple explanation to this: no band states exist below the band bottom, therefore, the spectral weight is shifted upwards due to the nonvertical transitions from the states above. Maybe what is surprising here is not that the vertical transition peaks have been shifted in energy but that, after the complicated many-body and surface effects are taken into account, the one-electron states can actually be identified rather accurately.

By following the ordinary vertical transition analysis we look for the local maxima in the calculated spectra. The peak positions (in circles) are illustrated in Fig. 5 as functions of $\hbar\omega$. They are to be compared with the measured results[6] (the crosses), and with the predicted transitions from an NFE band (the solid curves) and also from a quasiparticle band which includes the correction from Σ_1. The self-energy correction has two effects on the NFE bands: (1) the conduction band is narrowed and (2) a higher photon energy is, in general, needed for a vertical transition since[12] $\Sigma_1(k)-\Sigma_1(k_F)>0$ for $k>2k_F$. These effects are easily seen in Fig. 5 by comparing the solid and the dashed curves. The calculated result in general reproduces the quasiparticle band for states below -4 eV. The same is true in the measurement but only for $\hbar\omega > 85$ eV. For 30 eV $< \hbar\omega < 70$ eV, the measured peaks are generally 1–2 eV higher in energy than the quasiparticle band. This difference is much larger than the experimental resolution and cannot be understood readily. There are two possible explanations for the measured results. One is that the peaks are generally determined from vertical transitions. The measurement, then, suggests an anomalous k dependence of $\Sigma_1(k)$ in the final states; but this would be inconsistent with most self-energy calculations.[1,3,5,12] Another possibility is that a strong nonvertical transition greatly modifies the peak positions—an effect much larger than our calculation has suggested. Neither of the two explanations seem satisfactory. Detailed measurements at improved resolution in this energy range are necessary.

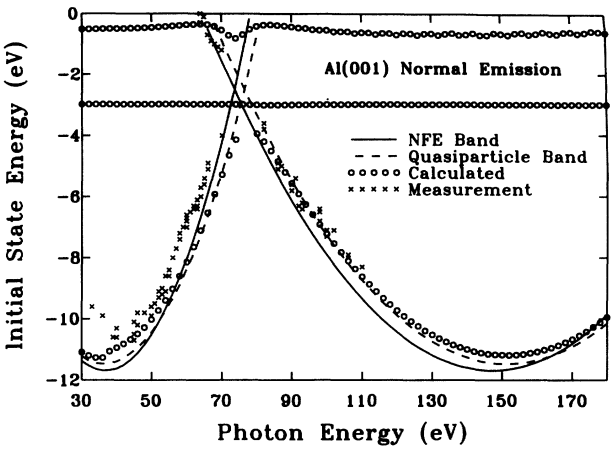

FIG. 5. The open circles indicate the peak positions from the calculated spectra at different photon energies. The results are expressed in terms of the initial-state energy. The crosses are from the measurement. The expected vertical transitions from the NFE band (the solid curve) and the quasiparticle band (the dashed curve) are also given.

Calculated spectra show a conduction bandwidth of 11.29 eV at $\hbar\omega = 34$ eV and of 11.20 eV at $\hbar\omega = 152$ eV, which are narrower than the quasiparticle band by 0.18 and 0.27 eV, respectively. This surface-related bandwidth reduction effect is small in Al. The same surface effect, however, was found to cause $\sim 10\%$ bandwidth narrowing in Na and K. There is a small difference in the calculated bandwidth at the two photon energies, which resulted from the difference in the final state MFP. A similar effect has also been found in the calculated Na spectral.[14] Such photon-energy dependence is small compared with the instrumental resolution and has yet to be verified experimentally.

The present study has included 0.22-eV bandwidth reduction due to the self-energy correction,[12] and has revealed an additional ~ 0.2-eV reduction due to a surface-related distortion that is intrinsic to photoemission measurements. So the calculated bandwidth is 11.25 eV, which is still 0.6–0.7 eV larger than the measured value of 10.6 eV. The difference might be explained by the scattering from the crystal potential. Band calculations predict that the one-body bands are narrowed by from 0.2 to 0.6–0.7 eV due to crystal scattering.[28–30] Therefore, with all the effects included, it is predicted that the bandwidth from photoemission measurements should be 10.8 ± 0.3 eV, which agrees with the measurement fairly well. The various bandwidth reduction factors are summarized in Table I. It should be noted that a recent self-energy calculation,[3] which includes vertex

corrections, predicts a 0.05-eV band narrowing for Al. This value is 0.17 eV smaller than the self-energy correction used in this study, but the difference would not offset the conclusion stated above.

Table I shows that the most important bandwidth reduction factor in Al comes from the crystal scattering, which is followed by an experimental artifact caused by a short MFP and by the self-energy correction. The state of the art of the so-called GW calculation has recently shown[2] that the combined effect of the lattice scattering and the self-energy correction (the real part only) leads to a large 1.7-eV band narrowing effect in Al—larger by 0.6 eV than the photoemission result. Mahan and Sernelius[3] has found that the proper inclusion of the vertex correction, which is neglected in the GW calculation, causes a substantial decrease in the band narrowing effect. This may explain the large discrepancy between our self-energy correction and the one from the GW method.

The bands above -2 eV (see Fig. 5) deserve further discussions. The peaks located at ~ -0.5 eV are mainly surface induced—as explained earlier. Vertical excitations are possible in the energy range 68 eV $<\hbar\omega<82$ eV, but they are strongly mixed with the surface-induced structure. The two structures cannot be separately identified from our calculation, where a 0.5-eV broadening effect has been included. The measured result at the same resolution, however, does show clearer band behavior here; even the band crossing at E_F has been determined. On the other hand, measured spectra (Fig. 4 of Ref. 6) look very similar to the calculated spectra (Fig. 3) and exhibit a similar structure at -0.5 eV in a wide range of photon energies. It seems that a measurement with improved resolution is needed for a better understanding of this -0.5-eV structure.

The surface state appears essentially stationary at -3 eV in Fig. 5. The evaluated surface-state intensity as a function of $\hbar\omega$ is illustrated in Fig. 6 (the solid curve), where the measured result (indicated by $\times$) is also given. Noticeably, there appears a resonance peak at $\hbar\omega\sim 76$ eV—where the vertical excitations from states near the band edge is predicted (see Fig. 5). This resonance is expected. As noted earlier, the surface state and the band-edge state have very similar momentum and energy. The momentum is $G/2$ at the band edge and is $G/2-iq$ (i.e., is complex) inside the gap. Thus, a resonant enhancement in the surface-state emission is expected near the photo-energy at which vertical transitions from states at $G/2$ take place. Such resonant behavior has been found

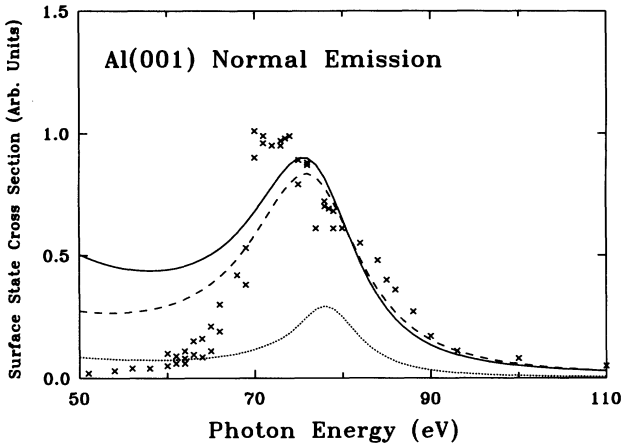

FIG. 6. The surface state cross section exhibits a resonance enhancement at $\hbar\omega\sim 76$ eV. The calculated result is given by the solid curve and the measured ones by the crosses. An analytical result from a simple two-band model are shown by the dashed curve. Band-edge state emission (for $k=G_{002}/2$) shows a similar resonance by calculation (dotted curve).

experimentally.[6] Similar resonance behavior has been discussed for the Cu(111) surface state.[31] Here, this effect is studied with a realistic calculation of the excitation matrix element. The calculation and the measurement agree fairly well on the high-energy side of the resonance, but they disagree appreciably on the low-energy side by a factor of ~ 30. A two-band calculation (the dashed curve) (see Appendix), also exhibits a similar discrepancy when compared with the measurement. The nature of the large intensity difference at low photon energies is not known and further studies are necessary.

The surface-state resonance might be related to the anomalous peak at E_F in the spectra of Na (Ref. 7) and K.[9] The dotted curves in Fig. 6 are calculated for band states near the band gap of Al; k is $G_{002}/2$. The resonance of the near edge states is very similar to that of the surface state, as can be expected from the early discussions. In alkaline metals, the Fermi level is very close to the zone boundary in the [110] direction. Thus, a similar resonant enhancement from the Fermi-level emission is possible in alkaline metals. Such an enhancement, however, must compete with an intensity reduction effect due to the Fermi-level cutoff. SM showed that the latter causes the Fermi-level emission intensity to decrease in

TABLE I. Various bandwidth reduction factors (in eV) of Al.

(1) Self-energy correction	(2) Intrinsic to photoemission	(3) Crystal scattering	(1)+(2)+(3)	Measurement
0.22[a]	0.18-0.27[b]	0.2; 0.7[c]	0.8±0.4	1.1[d]
0.05[e]		0.6[f]		
		0.7[g]		

[a]Reference 12.
[b]This calculation.
[c]Reference 28.
[d]Reference 6.
[e]Reference 3.
[f]Reference 29.
[g]Reference 30.

Na in the forbidden gap, i.e., where vertical excitation from an occupied state is not possible. In that calculation, the band-structure effect (i.e., the modification of the band dispersion and of the wave functions due to the lattice potential) was not included. The measured Fermi-level emission of K, however, has illustrated a resonant enhancement inside the forbidden gap.[9] How the band-structure effect, like the one that has been studied here for Al, affect the Fermi-level emission in the alkaline metals will be discussed in a planned future work.

III. CONCLUDING REMARKS

A theoretical study of the Al(001) normal emission spectra is presented, where the surface, the many-body and band-structure effects have been taken into account. General agreements with the measured result, especially with the spectral profiles, have been found. This result, together with SM's analysis of the Na spectra, provide a strong indication that these effects may be essential in the spectral analysis of other metals too.

A 0.2-eV band narrowing effect due to surface-induced distortion in photoemission has been identified. This effect, combined with the corrections due to the self-energy and the crystal potential scattering, could very well explain the measured 10.6-eV bandwidth of Al. It seems reasonable to conclude here that the conventional one-electron picture works for simple metals—provided that the complex self-energy and the band structure are included in the one-electron theory and that the surface effect is properly treated in photoemission.

The calculation shows that, at the 0.5-eV resolution, the quasiparticle band [or $\Sigma_1(k)$] of Al can be fairly accurately determined (Fig. 5). The measured result, however, agrees with the calculation only when $\hbar\omega > 85$ eV. A closer comparison at a better experimental resolution is needed for a better determination of $\Sigma_1(k)$ in the range, say, $0 < k < 5k_F$. This is important since there exist different many-body calculations that predict different self-energy corrections,[2,3,5] and there is a lack of experimental evidences to draw conclusions. High-resolution photoemission measurements can also be expected to reveal details of the surface-induced structure close to the Fermi level.

The calculated emission intensity from the surface state shows a resonant enhancement at $\hbar\omega \sim 76$ eV, which is observed experimentally. However, the calculation and the measurement differ seriously on the low-energy side of the resonance. Further studies are necessary to resolve this discrepancy. The relation of this resonance with the anomalous Fermi-level emission structure in Na and K has been briefly discussed. The possibility of a similar resonance in the Fermi-level emission of K is suggested. This problem is currently under investigation.

ACKNOWLEDGMENTS

This work was supported in part by the National Science Council of the Republic of China under Grants Nos. NSC 81-0208-M-007-09, NSC 82-0208-M-007-008, and NSC 83-0208-M007-041.

APPENDIX

In this appendix we employ the two-band model to describe states in the surface area. The results are analytic in form and are thus useful for studying the photoemission spectra, especially the surface-state emission.

The Hamiltonian for a crystal which occupies $z<0$ half space is approximated by

$$H=-\frac{1}{2}\frac{\partial^2}{\partial z^2}+V(z)\ , \tag{A1}$$

where

$$V(z)=(-V_0+V_{\pm G}e^{\mp iGz\mp iGd/2})\theta(-z)\ .$$

V_0 describes the potential step at the surface. The factor $e^{\mp iGd/2}$ accounts for the fact that the first layer has been put at $z=-d/2$. For convenience $V_G e^{-iGd/2}$ is denoted by $\bar{V}_G$. The wave functions satisfy $H\psi(z)=E\psi(z)$ with E relative to the vacuum level. The states in the flat, $z>0$ region are simply described by

$$\psi_p(z)=e^{ipz}+\mathrm{Re}^{-ipz} \text{ if } E>0 \text{ and } E\equiv\frac{p^2}{2}>0\ ,$$
$$\psi_\alpha=Be^{-\alpha z} \text{ if } E<0 \text{ and } E\equiv-\frac{\alpha^2}{2}\ . \tag{A2}$$

R and B are constants to be determined.

The standard two-band model for the $z<0$ region gives

$$\psi_k(z)=T\left[e^{ikz}+\frac{\bar{V}_G}{\mathcal{E}-\mathcal{E}_{k-G}}e^{i(k-G)z}\right]\ . \tag{A3}$$

$\mathcal{E}$ is the state energy inside the crystal (i.e., $\mathcal{E}-V_0=E$) and $\mathcal{E}_k=k^2/2$. T is to be determined. It is convenient to express $k=G/2+\eta$ in the gap region. The two-band mixing leads to the relation between η and $\mathcal{E}$:

$$\eta^2=f(\mathcal{E})\ , \tag{A4}$$

where

$$f(\mathcal{E})=2\mathcal{E}+2\mathcal{E}_{G/2}-2\sqrt{4\mathcal{E}\mathcal{E}_{G/2}+V_G^2}\ .$$

With proper boundary conditions at $z=0$, the states of (A1) at all energies can be determined from (A2)–(A4). States needed for evaluating Eq. (1) are the occupied state ($E<0$), ψ_k, and the scattering states ($E>0$), $\psi_p^>$. Surface states, occupied band states, and scattering states are discussed below.

1. Surface state ($E<0, f(E)<0$)

For $\psi_k(z)$ to remain finite in the $z<0$ region, it is necessary that

$$\eta=-i|f(\mathcal{E})|^{1/2}\equiv-iq\ , \tag{A5}$$

i.e., k is complex. It is convenient to rewrite (A3) for the surface states:

$$\psi_g(z)=T'e^{qz}\cos\left[\frac{G}{2}z+\delta\right]\ , \tag{A6}$$

which corresponds to

$$\cos 2\delta = (\mathcal{E} + \tfrac{1}{2}q^2 - \mathcal{E}_0)/\bar{V}_G \ ,$$

and

$$\sin 2\delta = -qG/2\bar{V}_G \ . \tag{A7}$$

A surface state at E is given by $\psi_\alpha(z)\theta(z) + \psi_g(z)\theta(-z)$, q and $\mathcal{E}$ satisfying (A5). Further, the continuity conditions of the wave functions of (A2) and (A6) at $z=0$ require that

$$\tan\delta = (q+\alpha)\frac{2}{G} \ . \tag{A8}$$

It follows from $\tan\delta > 0$ (i.e., $\sin 2\delta > 0$) that a surface state exists only if $\bar{V}_G < 0$. These results agree with the early two-band calculations.[32] A surface state of Al(001) is found at 2.6 eV below E_F, where we have taken $V_0 = 15.9$ eV (Fig. 1) and $2\bar{V}_{002} = -2V_{002} = -1.71$ eV as input parameters for (A6) and (A8).

2. The band state ($E < 0$, $f(E) > 0$)

The bounded bulk state is real and can be written as $\psi_k(z) + \psi_k^*(z)$ $(z < 0)$, where $\psi_k(z)$ is from (A3). With the proper boundary condition at $z = 0$,

$$T = \frac{B}{2}\left[\frac{1}{c} + i\frac{\alpha}{c'}\right] , \tag{A9}$$

where $c = 1 + \bar{V}_G/(\mathcal{E} - \mathcal{E}_{k-G})$ and $c' = k + (k-G)\bar{V}_G/(\mathcal{E} - \mathcal{E}_{k-G})$.

3. The scattering state ($E > 0$)

$\psi^>$ is a time-reversed LEED state,[19] which exists for $E > 0$. To take care of the Coulomb scattering experienced by the outgoing electron, k is a complex even if it is not inside not on the energy gap. Effectively, this means a non-Hermitian potential: $-i\Sigma_2(k)\theta(-z)$ ($-$ for time reverse) has been included in $V(z)$ of Eq. (A1). The constants T and R are determined from the continuity conditions at $z = 0$.

We need to replace $\mathcal{E} \to \mathcal{E} + i\Sigma_2$ in (A3) and (A4). Then, $f(\mathcal{E} + i\Sigma_2)$ in general is complex, and

$$\eta = \pm[f(\mathcal{E} + i\Sigma_2)]^{1/2} \ .$$

The $(\pm)$ is chosen so that $\mathrm{Im}(\eta) < 0$. One finds easily from (A2) and (A3):

$$R = \frac{pc - c'}{pc + c'}$$

and

$$T = \frac{2p}{pc + c'} \ , \tag{A10}$$

where $c = 1 + \bar{V}_G/(\mathcal{E} + i\Sigma_2 - \mathcal{E}_{k-G})$ and $c' = k + (k-G)\bar{V}_G/(\mathcal{E} + i\Sigma_2 - \mathcal{E}_{k-G})$. If $\bar{V}_G = 0$, (A10) reduces to the empty lattice result.[33]

With these two-band results, $\langle \psi_p^>(z)|\partial V(z)/\partial z|\psi_k(z)\rangle$ of Eq. (1) only involves elementary integrations and can be evaluated analytically. The surface-state emission cross section has been calculated and plotted in Fig. 6. The result from this two-band model agrees fairly well with that from a more detailed band calculation. Equations (A10) are also valid in the $\Sigma_2 \to 0$ limit, i.e., when the Coulomb scattering is neglected.

[1] L. Hedin and S. Lundqvist, Solid State Phys. **23**, 1 (1969).
[2] John E. Northrup, Mark S. Hybertsen, and Steven G. Louie, Phys. Rev. Lett. **7**, 819 (1987); Michael P. Surh, John E. Northrup, and Steven G. Louie, Phys. Rev. B **38**, 5976 (1988); John E. Northrup, Mark S. Hybertsen, and Steven G. Louie, *ibid.* **39**, 8198 (1989).
[3] G. D. Mahan and B. E. Sernelius, Phys. Rev. Lett. **62**, 2718 (1989).
[4] H. O. Frota and G. D. Mahan, Phys. Rev. B **45**, 6243 (1992).
[5] H. Yasuhare and Y. Ousaka (unpublished).
[6] H. J. Levinson, F. Greuter, and E. W. Plummer, Phys. Rev. B **27**, 727 (1983).
[7] E. Jensen and E. W. Plummer, Phys. Rev. Lett. **55**, 1912 (1985).
[8] I. W. Lyo and E. W. Plummer, Phys. Rev. Lett. **60**, 1558 (1988).
[9] B. S. Itchkawitz, I.-W. Lyo, and E. W. Plummer, Phys. Rev. B **41**, 8075 (1990).
[10] K. W.-K. Shung and G. D. Mahan, Phys. Rev. Lett. **57**, 1076 (1986).
[11] K. W.-K. Shung and G. D. Mahan, Phys. Rev. B **38**, 3856 (1988).
[12] K. W.-K. Shung, B. Sernelius, and G. D. Mahan, Phys. Rev. B **36**, 4499 (1987).
[13] K. W.-K. Shung and Shih-Kuei Ma, Chin. J. Phys. **28**, 49 (1990).
[14] K. W.-K. Shung, Phys. Rev. B **44**, 13 112 (1991).
[15] A. W. Overhauser, Phys. Rev. Lett. **55**, 1916 (1985).
[16] J. H. Kaiser, J. E. Inglesfield, and G. C. Aers, Solid State Commun. **63**, 689 (1987).
[17] W. Kohn and L. J. Sham, Phys. Rev. **140**, A1133 (1965).
[18] N. D. Lang and W. Kohn, Phys. Rev. B **1**, 4555 (1970).
[19] G. D. Mahan, Phys. Rev. B **2**, 4334 (1970).
[20] P. J. Feibelman, Phys. Rev. B **12**, 1319 (1975); Harry J. Levinson and E. W. Plummer, *ibid.* **24**, 628 (1980).
[21] N. W. Ashcroft, Phys. Lett. **23**, 48 (1966).
[22] J. E. Inglesfield, Rep. Prog. Phys. **45**, 276 (1982).
[23] P. A. Serena, J. M. Soler, and N. García, Phys. Rev. B **37**, 8701 (1988).
[24] J. K. Grepstad *et al.*, Surf. Sci. **57**, 348 (1976).
[25] G. D. Mahan, *Many-Particle Physics* (Plenum, New York, 1981), Chap. 6.
[26] B. E. Sernelius, Phys. Rev. B **33**, 8582 (1986); **34**, 5610 (1986).
[27] S. Y. Tong and T. N. Rhodin, Phys. Rev. Lett. **26**, 711 (1971).
[28] F. Szmulowicz and B. Segall, Phys. Rev. B **24**, 892 (1981).
[29] S. P. Singhal and J. Callaway, Phys. Rev. B **16**, 1744 (1977).
[30] M. Seel, Phys. Rev. B **28**, 778 (1983).
[31] S. G. Louie, P. Thiry, R. Pinchaux, Y. Petroff, D. Chandesris, and J. Lecante, Phys. Rev. Lett. **44**, 549 (1980).
[32] F. Forstmann, Z. Phys. **235**, 69 (1970).
[33] W. L. Schaich and N. W. Ashcroft, Phys. Rev. B **3**, 2452 (1971).